BRAIN CONNECTIVITY
Volume 13, Number 7, 2023

DOI: 10.1089/brain.2022.0077

Effect of Extremely Preterm Birth on Adolescent Brain Network Organization

M. Fiona Molloy,[1] Emily J. Yu,[1] Whitney I. Mattson,[2] Kristen R. Hoskinson,[2] H. Gerry Taylor,[2,3] David E. Osher,[1] Eric E. Nelson,[2,3] and Zeynep M. Saygin[1]

Abstract

Introduction: Extremely preterm (EPT) birth, defined as birth at a gestational age (GA) <28 weeks, can have a lasting impact on cognition throughout the life span. Previous investigations reveal differences in brain structure and connectivity between infants born preterm and full-term (FT), but how does preterm birth impact the adolescent connectome?

Methods: In this study, we investigate how EPT birth can alter broadscale network organization later in life by comparing resting-state functional magnetic resonance imaging connectome-based parcellations of the entire cortex in adolescents born EPT ($N = 22$) to age-matched adolescents born FT (GA ≥37 weeks, $N = 28$). We compare these parcellations to adult parcellations from previous studies and explore the relationship between an individual's network organization and behavior.

Results: Primary (occipital and sensorimotor) and frontoparietal networks were observed in both groups. However, there existed notable differences in the limbic and insular networks. Surprisingly, the connectivity profile of the limbic network of EPT adolescents was more adultlike than the same network in FT adolescents. Finally, we found a relationship between adolescents' overall cognition score and their limbic network maturity.

Discussion: Overall, preterm birth may contribute to the atypical development of broadscale network organization in adolescence and may partially explain the observed cognitive deficits.

Keywords: adolescents; connectivity; connectome; fMRI; preterm birth; resting state

Impact Statement

Extremely preterm (EPT) birth is associated with persistent cognitive and behavioral impairments throughout the life span. Previous research in infants has revealed altered resting-state networks due to EPT, but are these differences also observed in adolescence? In this study, we compare brain-wide parcellations based on patterns in functional connectivity in EPT and full-term adolescents. We found differences in the insula and limbic network, where EPT adolescents show a more adultlike limbic network, and the maturity of personalized limbic networks may predict cognition. These results highlight the effect of preterm birth on brain network organization well beyond infancy.

[1]Department of Psychology, The Ohio State University, Columbus, Ohio, USA.
[2]Center for Biobehavioral Health, Abigail Wexner Research Institute, Nationwide Children's Hospital, Columbus, Ohio, USA.
[3]Department of Pediatrics, Ohio State University College of Medicine, Columbus, Ohio, USA.

Effect of Extremely Preterm Birth on Adolescent Brain Network Organization

Although mortality rates for preterm birth have improved substantially in recent years, substantial levels of morbidity persist. More extreme degrees of preterm birth, whether defined as very preterm (VPT, gestational age [GA] <32 weeks) or extremely preterm (EPT, GA <28 weeks), are associated with functional impairment throughout the life span. Even VPT infants with low medical risk exhibit alterations in neurobehavior (Pineda et al., 2022). By the time EPT born children enter school, they exhibit cognitive deficits in a wide range of domains, including language, motor and perceptual motor skills, spatial and nonverbal reasoning, and executive functions (Orchinik et al., 2011), as well as global reductions in intelligence quotient (IQ) (Pascoe et al., 2021). Such cognitive deficits contribute to diminished academic outcomes such as mathematical and reading performance (Aarnoudse-Moens et al., 2009; Pascoe et al., 2021).

In general, greater cognitive impairments are observed in children born at a lower GA (Kerr-Wilson et al., 2012). However, even in individuals born during the late preterm period (GA 34–36 weeks), childhood deficits on neurocognitive tests are evident and deficits can perpetuate into late adulthood (Heinonen et al., 2015).

In addition to specific cognitive difficulties, children born EPT or VPT display differences in large-scale personality traits (e.g., higher agreeableness and conscientiousness) (Pesonen et al., 2008) and more problems in social cognition and social-behavioral outcomes (e.g., Theory of Mind) (Fu et al., 2022; Taylor, 2020) relative to term born, or full-term (FT, GA ≥37 weeks) counterparts. This combination of both cognitive and functional difficulties can result in long-term consequences on socioeconomic outcomes and quality of life (e.g., income and whether an individual starts a family) (Moster et al., 2008). Finally, children and adults born VPT exhibit increased rates of meeting the criteria for psychiatric disorders, particularly for autism spectrum disorder (ASD) and attention-deficit/hyperactivity disorder (ADHD) (Anderson et al., 2021).

Persistent cognitive and behavioral impairments of preterm born youth are likely a reflection of altered neural function. Given the protracted process of postnatal brain development, such deficits may reflect both the persistent impact of neural impairments present at birth (e.g., leukomalacia) and ongoing alterations in the trajectory of neurodevelopment across childhood and adolescence. Identifying the patterns of brain engagement in preterm children at the network level may help inform the specific nature and developmental patterns that underscore these wide-reaching and persistent deficits in socioemotional and cognitive functioning.

Previous neuroimaging research has revealed neural differences early in life between infants born FT and preterm. These differences appear distributed across the brain, as supported by alterations in structure (e.g., gray matter volume), functional connectivity (cofluctuations in functional magnetic resonance imaging [fMRI] BOLD signal), and structural connectivity (e.g., fractional anisotropy measured using diffusion-weighted imaging). Compared with infants born FT, those born preterm show decreased gray matter volume in cortical and subcortical regions, widely distributed lesions in white matter, and increased levels of cerebrospinal fluid (CSF) (Inder et al., 2005). The severity of abnormalities in the brain structure of preterm infants is predictive of cognitive deficits at 18 months (Dimitrova et al., 2021) and even later in childhood at 8 years (Anderson et al., 2015).

Relatedly, studies using diffusion-weighted imaging show that infants born preterm exhibit reduced structural connectivity, including reduced fractional anisotropy in key structures and tracts of the brain, such as the genu of the corpus callosum (Anjari et al., 2007), and disruptions in network architecture (Ball et al., 2014; de Almeida et al., 2020) and local connections (Batalle et al., 2017). These early neural differences may also explain the behavioral differences seen later in life. For example, differences in the structure of thalamocortical circuits (due to preterm birth) in infancy significantly predicted group differences in cognitive scores at age 2 (Ball et al., 2015; Ball et al., 2013). A similar pattern has also been reported with other measures of white matter connections, particularly of frontal areas, in which reductions in preterm infants could predict cognitive scores at age 2 (Girault et al., 2019).

Finally, infants born preterm also exhibit disrupted functional connectivity in resting-state studies, including reduced connectivity between hubs (Scheinost et al., 2016), absence of some resting-state networks (Doria et al., 2010), and brain-wide disruptions in all resting-state networks (Eyre et al., 2021). These disruptions appear to persist past the neonatal period, with weaker connections in resting-state networks at 3 years in children born preterm (Damaraju et al., 2010).

Do the well-documented neural differences in infancy also continue throughout development and explain behavioral differences that persist throughout adolescence? Previous studies in adolescents and young adults born VPT have identified structural differences in both gray and white matter volume using MRI (Karolis et al., 2017; Nosarti et al., 2014; Nosarti et al., 2008). Furthermore, seed-based connectivity analyses based on adult networks have shown brain-wide differences in connections where functional connectivity tended to be weaker for adolescents born VPT (Wehrle et al., 2018), but even children born late preterm exhibited altered structural and functional connectivity in late childhood and early adolescence, including *increased* levels of connectivity in some regions (Degnan et al., 2015), perhaps reflecting a compensatory response. However, the differences in broadscale functional organization specific to adolescents have not yet been extensively explored.

In children born preterm, previous studies have found a link between brain metabolism and executive function (Schnider et al., 2020) and gray matter volume and mathematical ability (Collins et al., 2022). In addition, studies of adolescents born preterm have demonstrated a link between adolescent brain structure and cognitive outcomes (Cheong et al., 2013; Karolis et al., 2017; Nosarti et al., 2008), but the link between adolescent resting-state connectivity and cognitive and behavioral deficits due to preterm birth remains unclear (Wehrle et al., 2018).

Broadscale functional organization or brain-wide network connectivity can be gleaned from parcellating the cortex into distinct networks based on features such as structural or functional connectivity and assessing network connectivity across the entire brain. In adults, numerous parcellations describe broadscale organization based on functional connectivity (Arslan et al., 2018; Eickhoff et al., 2018).

Characterizing adolescent-specific broadscale organization is ideal for exploring differences due to preterm birth because of the following: (1) it can capture network organization across development and capture individual differences in connectivity; (2) it can capture these differences across the entirety of cortex, including both local and long-range connections; (3) broadscale connectivity is closely related to behavior (Kong et al., 2019; Rosenberg et al., 2016); and (4) disruptions in functional connectivity and network organization are linked to neurological and psychological disorders (Buckholtz and Meyer-Lindenberg, 2012; van den Heuvel and Sporns, 2019). Because cognitive differences due to preterm birth persist throughout adolescence (Johnson and Marlow, 2017), and given the close relationship between broadscale functional brain organization and behavior, it follows that neural differences in this organization may also be present in adolescence (and may explain some of the cognitive differences observed).

In this study, we compare brain-wide parcellations of resting-state activity in adolescents born EPT and an age-matched group of FT adolescents based on patterns in functional connectivity (vertex-wise connectome). First, we compute and compare the broadscale network organization (Fig. 1) of data collected on EPT and FT adolescents using a method we implemented on infant connectomes (Molloy and Saygin, 2022). The EPT and FT connectomes are constructed based on the vertex-to-vertex functional connectome at rest. *k*-Means, an unsupervised machine learning algorithm, parcellates this matrix by grouping together vertices with similar connectivity profiles into a network. Unlike other approaches, we use entire high-resolution connectomes to define adolescent-specific functional networks without seeding anatomical regions. The optimal solutions are identified and compared between the EPT and FT groups.

Second, we compare the adolescent networks with the adult networks using a large-scale and widely used parcellation of adult resting-state data (Yeo et al., 2011). Third, we compute individualized adolescent parcellations and explore how adultlike networks relate to age-corrected scores of overall cognition.

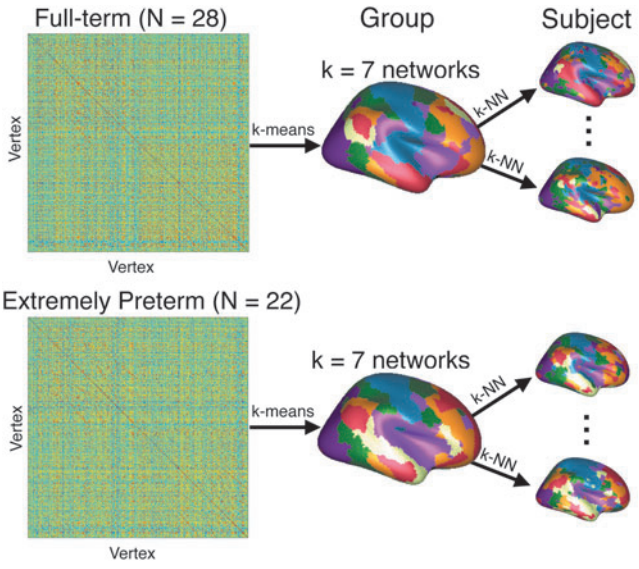

FIG. 1. Schematic of parcellation method. Adolescent brain network organization in EPT ($N=22$) and FT ($N=28$) adolescents was characterized by parcellating the brain based on resting-state functional connectivity. In both groups of adolescents, the underlying high-resolution vertex-by-vertex connectomes were parcellated using *k*-means. The optimal $k=7$-network solution is shown. Individual solutions were computed based on the left-out-subject's group solution using k-NN classification. EPT, extremely preterm; FT, full-term; k-NN, k-nearest neighbor.

Methods

Participants

Two groups of adolescents, ages 11–16 years, were recruited. Adolescents born EPT were recruited from chart reviews of age-wise eligible individuals born EPT in one of the neonatal intensive care units within a neonatal network of a large children's hospital in the Midwest, USA. From among those with GA <28 weeks who lived within the region served by the hospital, adolescents were divided into subsets according to age. Contacts with families were in cycles, with the family of a youth within each age subset enrolled before moving the next cycle of recruitment, until reaching a sample quota of 24 youth. To be eligible, youth and their families had to have proficiency in English and youth had to be free of severe sensory impairment and conditions other than preterm birth that would place them at high risk for severe developmental disability (e.g., ASD, intellectual impairment, genetic disorders).

Youth born FT ages 11–16 years were recruited from postings for research volunteers using similar exclusionary criteria. Participants included some sibling pairs (two in the EPT group and three in the FT group). The study was approved by the hospital's IRB, and both caregiver consent and youth assent were obtained before participation.

The total sample included 24 adolescents born EPT and 29 born FT. Three participants were excluded from this study due to lack of a functional scan or registration issues, described below. The final sample used to define the brain networks included 50 adolescents: 22 adolescents born EPT (mean age at scan: 13.86 years; age range at scan: 11.43–16.93 years; 11 males and 11 females) and 28 age-matched adolescents born FT (mean age at scan: 13.84 years; age range at scan:11.17–16.74 years; 14 males and 14 females). Demographic details are summarized in Table 1. Full demographic statistics are detailed in Supplementary Table S1.

Acquisition

The adolescents were scanned using a Siemens Prisma 3T scanner with a 64-channel head coil with simultaneous multislice acquisition enabled located in the hospital section of neuroradiology. High-resolution T1-weighted magnetization prepared gradient echo (MPRAGE) and T2*-weighted echo planer images (EPI) were collected for all subjects. Sequence parameters for the MPRAGE were as follows: 160 sagittal slices, 1 mm^3 voxels, TE/TR = 62/2300 ms; FOV = 240 mm^2. The EPI parameters were as follows: 36 axial slices, $2.55\times2.55\times4$ mm voxels; TE/TR = 30/1500. Each individual's resting-state scan consisted of 246 volumes (6.15 min), acquired during eyes open and fixating on visually projected crosshairs.

Table 1. Demographics of Adolescents

Group	Sample size	Chronological age, years	Gestational age, weeks	Birth weight, g	Socioeconomic status, z-scored
All	50	13.8 ± 1.8	33.2 ± 6.9[a]	2180.5 ± 1307.8[b]	−0.00045 ± 1.04
EPT	22	13.9 ± 1.9	25.9 ± 1.2	854.4 ± 283.8	−0.37 ± 0.97
FT	28	13.8 ± 1.7	39.3 ± 1.1[a]	3347.5 ± 420.8[b]	0.29 ± 1.01

Values in table are mean ± standard deviation.
[a]Two individuals missing data.
[b]Three individuals missing data.
EPT, extremely preterm; FT, full-term.

Preprocessing

Cortical reconstruction was performed using the recon-all pipeline in the FreeSurfer image analysis suite 6.0 (http://surfer.nmr.mgh.harvard.edu/), as described in Fu et al. (2022). Resting-state data were registered to native anatomy with bbregister, and preprocessing included slice to volume correction, spatial smoothing, interpolation over motion spikes, and bandpass filtering (0.009–0.08 Hz). Frames were censored from the data if there was >1 mm of total vector motion and included framewise displacement as a motion regressor. We generated masks of white matter, CSF, and subcortical structures for each subject in their native anatomical space using FreeSurfer's parcellation, and performed denoising using the CSF and white matter masks. One individual in the EPT group was excluded because of poor registration to the FreeSurfer6 template space.

Defining the connectome

Broadscale networks were computed from high-resolution connectomes that describe functional connectivity, or pairwise coactivation between surface vertices of the brain. We quantified functional connectivity as the pairwise Pearson correlation between each vertex's z-scored time series. An individual's resting-state data were first downsampled to the FreeSurfer5 template resulting in 18,742 vertices. Connectomes were then defined for each individual (18,742 × 18,742 matrix). Next, group average connectomes were defined separately for the EPT and the FT groups. For the group average connectomes, individual connectomes were transformed using the Fisher r to z transform, averaged across the group, and then transformed back using the inverse Fisher z to r transform.

To ensure generalizability of these solutions with a smaller sample size, this procedure was rerun using a leave-one-out method where a single subject was excluded. For example, the EPT group had 22 group connectomes, where each connectome was calculated by averaging across 21 individual connectomes, leaving out a single subject iteratively. The final solution used to compare networks between groups and to adults included all individuals within a group.

Defining group-level networks

Broadscale functional networks were defined using k-means clustering. k-Means parcellates the connectome into k-networks comprising vertices with similar connectivity profiles. Similarity was measured by the correlation of vertex-wise connectivity profiles, in line with similar approaches in infants and adults that also utilize this measure, as it does not just reflect differences in signal-to-noise ratios (Molloy and Saygin, 2022; Yeo et al., 2011). k-Means solutions were all replicated 100 times to ameliorate the influence of initialization of starting values on the resulting networks (Fränti and Sieranoja, 2019).

While k-means is a data-driven algorithm, the total number of networks (or k) must be specified by the user. While there is not necessarily a single correct solution, some values of k are more appropriate than others. To identify optimal solutions, we calculated solutions along an entire sequence of $k = 2$–25 networks for the EPT and FT groups. We first identified the optimal solutions using the $N-1$ group connectomes described above to maximize our confidence in the stability of these parcellations.

To find optimal solutions, these group parcellations were evaluated based on two metrics: fit to data and stability. First, an optimal solution should fit the underlying data well. In other words, the connectivity patterns of vertices within the same network should be as similar as possible, while the differences between connectivity patterns of vertices in different networks should be maximized. The underlying data here are the left-out individual's connectome. The clusters, or parcel assignments for each vertex, are defined by the group connectome (EPT or FT) for all of the other individuals within that group. We quantify fit to data using the silhouette coefficient (SC), where a higher SC indicates a better fit. The SC is defined as follows:

$$SC_k = \frac{a_k - b_k}{\max(a_k, b_k)}$$

where a is the functional homogeneity within cluster k, and b is the functional homogeneity between vertices in cluster k and other clusters.

The within-cluster functional homogeneity, a, is defined as follows:

$$a_k = \frac{\sum_{i,j;i\neq j} \mathrm{corr}(v_i, v_j)}{n_k(n_k - 1)}$$

where n_k denotes the number of vertices in cluster k, corr (v_i, v_j) is the correlation between vertex i and vertex j, and i and j range from 1 to n_k. Between-cluster homogeneity, b, is defined as follows:

$$b_k = \frac{\sum_i \sum_x \mathrm{corr}(v_i, v_x)}{n_k(N - n_k)}$$

where $\mathrm{corr}(v_i, v_j)$ is the correlation between vertex i and vertex j, n_k denotes the number of vertices in cluster k, and N

represents the total number of vertices. i and j range from 1 to n_k, and x ranges from 1 to $N - n_k$.

Second, the $N-1$ group solutions should be stable across all other $N-1$ group solutions within each group. In other words, we do not want to overfit the data, so the solutions should not differ much if different individuals are excluded. We quantify stability with the Dice index, which measures the overlap between two solutions (Dice, 1945). The Dice index ranges from 0 to 1, where 0 denotes no overlap and 1 denotes perfect overlap. A larger Dice index then signifies greater stability when different individuals are left out of calculation. Dice is defined as follows:

$$\mathrm{DICE}_k = \frac{2\,|X_k \cap Y_k|}{|X_k||Y_k|}$$

where $|X_k \cap Y_k|$ is the number of vertices in both parcel X_k and parcel Y_k, $|X_k|$ is the total vertices in X_k, and $|Y_k|$ is the total vertices in Y_k. Dice is computed for pairs of parcels without replacement, and we use the overall Dice for most comparisons by averaging across all networks. Optimal networks were identified based on solutions of k total networks that maximized SC and Dice. For visualization only, the optimal solutions are smoothed slightly using morphological opening (one step of dilate followed by one step of dilation, to preserve shape of networks) and plotted on the surface.

The confidence of the optimal solution for both groups is computed based on similar methods in parcellation of resting-state connectivity of children (Tooley et al., 2022) and adults (Yeo et al., 2011). Confidence ranges from -1 to 1, where 1 indicates higher confidence and is defined as follows:

$$\mathrm{Confidence}_i = \frac{b_i - a_i}{\max(a_i, b_i)}$$

where a_i is the mean distance (correlation of connectivity profiles) between vertex i and all vertices within that same network, and b_i is the mean distance between vertex i and all vertices assigned to a different network. This measure is similar to SC, but uses pairwise distances and computes a value for each vertex, instead of for each network.

Defining subject-level networks

From the centroids of the optimal group-level networks, we define individualized parcellations using k-nearest neighbor classification following a similar approach for neonate individual solutions in Molloy and Saygin (2022). Briefly, for a given subject, we assign each vertex to a network according to which network has the closest centroid, or the most similar mean connectivity profile. Critically, the group centroids are defined from the $N-1$ parcellation (not including that subject), that is, the group and subject data are independent when defining individual solutions. The individual solutions are smoothed slightly using morphological opening (one step of dilate followed by one step of dilation, to preserve shape of networks), as the individual data are noisier than the group data.

Eight individuals in total (four FT and four EPT) were excluded from comparison with adults and the regression analyses because of lack of data (possibly due to noise) in some networks (i.e., if one of the seven networks only included a few, if any, vertices; see Supplementary Fig. S4). However, we include analyses with the entire data set (no exclusions), and we find the results are replicated (Supplementary Table S3 and Supplementary Fig. S6).

Comparing parcellations between groups and with adults

First, we compare the EPT and FT group solutions using the Dice coefficient above. The Dice coefficients are reported for paired networks (sorted by highest overlap across the two solutions) and for the entire k solution calculated from the entire group (e.g., based on the average connectome for all 22 EPT adolescents and the average connectome for all 28 FT adolescents). To interpret the magnitude of the between-group Dice, we use bootstrapping to construct a null between-group distribution. We randomly sample (with replacement) two groups while accounting for the differences in group size.

We create a null $N=28$ sample with 14 randomly selected EPT and 14 FT adolescents, and a null $N=22$ sample with 11 EPT and 11 FT adolescents. From these null samples, we compute the group connectomes, find the $k=7$ (optimal) solutions, and calculate the Dice coefficient between groups. This procedure is repeated 500 times for a total of 500 bootstrap samples.

Second, to determine how adultlike the EPT or FT optimal solutions are, we compare the $k=7$-network adolescent networks to adult seven-network solution from Yeo et al. (2011) using the Dice coefficient. The adult seven-network Yeo (liberal mask) solution in Montreal Neurological Institute space was downloaded from https://surfer.nmr.mgh.harvard.edu/fswiki/CorticalParcellation_Yeo2011. We also compare the individual parcellations to the seven-network Yeo solution. The Yeo networks are first matched to the $N-1$ parcellation, and then those labels are used for the individual to adult comparison.

Finally, we conducted an exploratory analysis to see if an *individual's* overlap with the adult limbic network (the network that contained the largest between-group difference) corresponds to cognitive functioning. Our behavioral measure of interest is the (age-adjusted) cognition total composite score from the NIH Toolbox (Casaletto et al., 2015). This total composite score includes the composite scores for both crystallized and fluid intelligence across the domains of executive functioning, episodic and working memory, language, processing speed, and attention. We defined a linear model (referred to as the ''reduced'' model) with main effects of group membership (EPT or FT), limbic network Dice, and an interaction term of group × overlap, or

$$Y_{\mathrm{Cognition}} \sim \beta_1 Limbic + \beta_2 EPT + \beta_3 Limbic * \mathrm{EPT}$$

A ''full'' model was also fit, building upon the above model and adding a main effect for standardized socioeconomic status, or

$$Y_{\mathrm{Cognition}} \sim \beta_1 Limbic + \beta_2 EPT + \beta_3 Limbic * \mathrm{EPT} + \beta_4 \mathrm{SES}$$

The Bayesian information criterion (BIC) (Schwarz, 1978) was used to compare model fit penalized by complexity. Note that 42 individuals are included in the regression analysis. Supplementary Table S2 shows the demographic details of these 42 individuals. These individuals were identified based on the visual inspection of the individual

solution, excluding those with a network containing no vertices, or those with a majority of vertices assigned to a single network (Supplementary Fig. S4). The eight excluded subjects (four FT, four EPT) had a significantly higher median framewise displacement than the included subjects (rank sum test, $p = 0.0221$; see Supplementary Fig. S5 for full distribution). These modeling results are replicated in Supplementary Table S3 and Supplementary Figure S6 with all 50 subjects, including those 8 subjects with noisier individual solutions.

Results

Differences in functional networks in adolescents born preterm

We first describe the functional organization of the brain of adolescents born EPT and born at FT. EPT and FT parcellations were determined using a leave-one-subject-out procedure, where we calculated the average connectome among the rest of the subjects, defined clusters based on *k*-means clustering, and identified the optimal solution. Because the approach for defining networks is data-driven, we made no *pre hoc* assumptions on the total number of networks (k) to include, and determine the optimal k based on which solution best captures the data while maintaining stability. This optimal k-network solution was determined by identifying which k had a high SC (good fit to data) and high Dice coefficient between left out solutions (high stability). The SC and Dice coefficients for each k from 2 to 25 networks for each group are shown in Figure 2.

An SC >0.90 was shown in solutions with a k of 6 or greater, and so, we determined that any solution with 6 or more networks had a sufficiently high fit to data. Stability was determined by identifying local maximums in mean Dice coefficients. Based on these criteria, the EPT group had optimal solutions of $k = 7$, 8, 12, and 15, while the FT group had optimal solutions with $k = 5$, 6, 7, 9, 12, and 16 networks. In this study, we focus on the seven-network solution, as it was an optimal solution in both groups of adolescents. In addition, previous work suggests that a seven-network solution is optimal for adults (Yeo et al., 2011), allowing for a straightforward comparison between our adolescents here and the previously released adult network solution.

Furthermore, a seven-network solution has been described for other age groups, including infants (Molloy and Saygin, 2022) and children (Tooley et al., 2022), thus providing a comparison for this data set. We also include all optimal solutions (not just seven-network solutions) for both age groups plotted on the surface in Supplementary Figure S1.

Figure 3a displays the seven-network solutions for the adolescents born EPT and FT. The networks were named based on the closest, that is, most overlapping, network in the Yeo et al. (2011) seven-network solution. The adolescent seven-network solution contained both local (network comprised a single component in a continuous area) and distributed (network comprised two or more noncontiguous clusters) networks for both groups, which were largely symmetric across hemispheres. The local networks were in areas of the occipital (visual network) and motor (somatomotor) cortices. The overall between-group Dice is 0.64, which was significantly lower than the mean of the null between-group bootstrapping distribution (two-sided one-sample t-test: $t(499) = 8.29$, $p = 1.09 \times 10^{-15}$; Supplementary Fig. S2), however, 31.8% of the bootstrapped samples were above 0.64, suggesting that the observed between-group Dice is an above average, but not a significant group difference ($p = 0.32$).

The largest differences between groups were found in some of the distributed networks in association areas, but this value varied depending on the network. Figure 3b shows the quantitative comparison broken up by network.

The largest discrepancy between the networks of the two groups is shown in dark red, or the proto-limbic network.

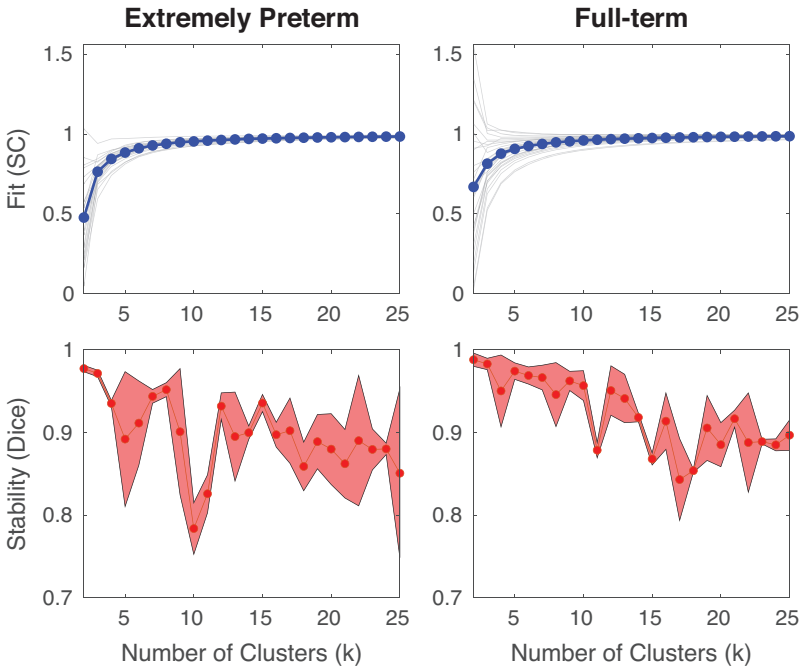

FIG. 2. Optimal solutions. The fit to data and stability for each solution are shown for the adolescents born EPT (left column) and adolescents born FT (right column). The first row shows the fit to the left-out data (SC; y-axis) for each k solution (y-axis). The gray lines are for individual subjects and the blue dots denote the group average. The second row shows the stability (quantified by the Dice coefficient) of the left-out group solutions. The red line/points show the mean of the within-group overlap and the shaded regions show ±1 standard deviation. SC, silhouette coefficient.

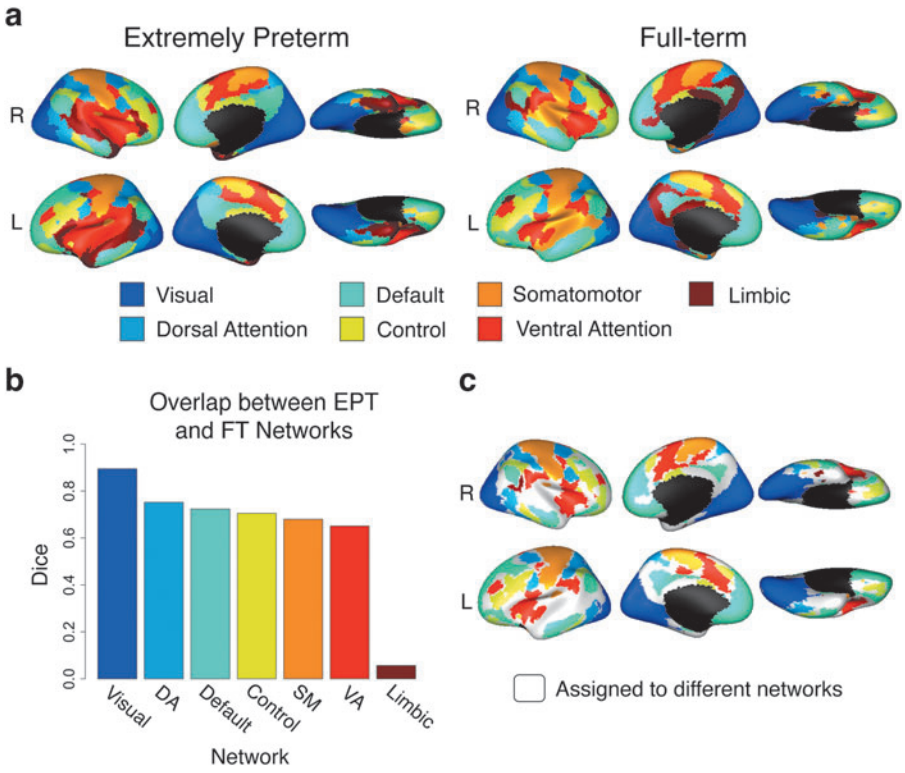

FIG. 3. Preterm and FT networks. **(a)** The seven-network optimal solutions for the adolescents in the EPT group and the FT group. The colors are assigned based on the matched networks from the Dice coefficient. **(b)** The quantitative overlap between the networks color-coded by the networks in **(a)**. Higher Dice indicates higher overlap. **(c)** The white regions indicate vertices assigned to different networks in the EPT and FT seven-network solutions.

In the FT group, the ''limbic'' network's main component was in the posterior cingulate cortex. However, in the EPT group, the limbic network was mainly confined to the temporal lobe. Another key difference between groups is in the insula. In the FT group, the insula was part of the somatomotor network, whereas in the EPT group, it was included as part of the ventral attention network, separate from the somatomotor network.

While most differences between groups were in the insular and posterior cingulate cortex, there were differences all throughout the brain, especially in the borders between networks. Figure 3c illustrates the vertices assigned to different networks in the EPT and FT groups. A total of 6100 vertices (32.55% of total vertices) were assigned to different networks in the EPT and FT solutions.

Overall, the confidence of the adolescent seven-network solutions was similar to the confidence observed in seven-network solutions for children (Tooley et al., 2022) and for adults (Yeo et al., 2011). Confidence plotted on the surface and averages per network are shown in Supplementary Figure S3. Similar to results from previous work (for both adult and child solutions), the EPT and FT adolescent solutions had qualitatively higher confidence in the primary cortex (particularly occipital cortex) than in the association areas (particularly in inferior frontal and temporal regions). In addition, the confidence of boundary vertices on the edge of networks tended to be lower. The FT group exhibited low confidence in regions such as the precuneus, similar to the clustering confidence in children (Tooley et al., 2022), while the EPT group exhibited relatively higher confidence in that region, more closely resembling the adult solution.

These results suggest that confidence in the adolescent clustering solutions fall between what was previously observed in adults and children, and that EPT adolescents display accelerated development in these regions.

Because the results of k means are governed by the user's choice of k, we investigated the consistency of the differences we observed between groups, specifically for the posterior cingulate and insula. For example, it is plausible that a posterior cingulate network would also emerge in the EPT group if a different solution was selected. In fact, as shown in Supplementary Figure S1, the $k = 8$ EPT solution has a network that contains a posterior cingulate component (PCC) and resembles the so-called limbic network identified in the optimal seven-network FT solution. Are these network differences between FT and EPT consistent across multiple resolutions of k? If so, it would indicate a more robust and reliable group difference.

To quantitatively determine which networks are consistently delineated across higher k, we conducted a boundary analysis by identifying how many times a given vertex makes up a network boundary across the $k = 8$ to 25-network solutions. All k are included to eliminate any experimenter assumptions, as the choice of k is relative and subjective. In this analysis, if a vertex is frequently a boundary, it represents a transition point between different networks. Conversely, if an area of cortex contains vertices that are rarely, or never, boundaries across k, it suggests that this region has quite homogenous connectivity profiles. These are vertices that are a single cluster no matter how many chances you give the algorithm to divide it up into subclusters. Their connectivity profiles are so highly similar to each other and highly dissimilar to other networks that they are not split into multiple networks (even at high k).

The results of this analysis are shown in Figure 4a, which illustrates the number of times a given vertex is a boundary

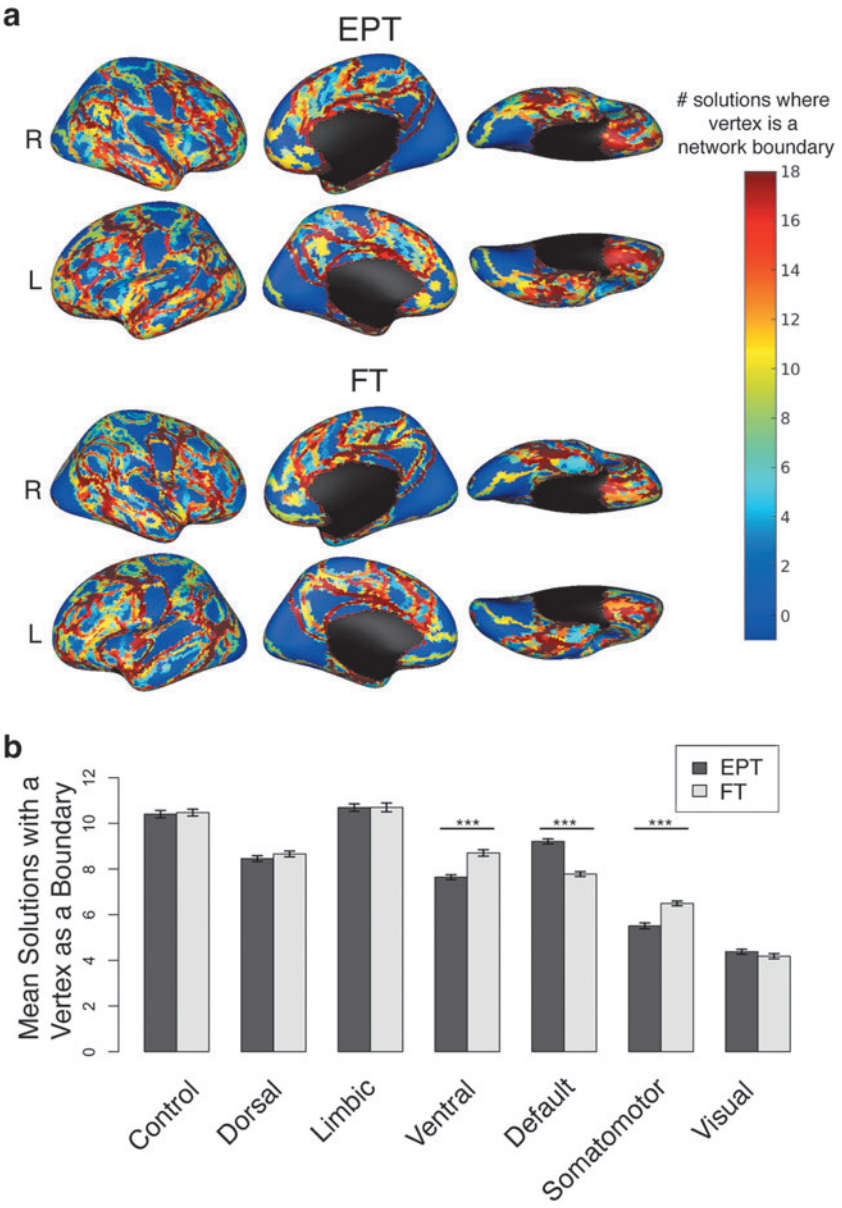

FIG. 4. Further subdivisions of seven-network solutions. **(a)** The number of times a vertex is a boundary in k solutions higher than 7 is shown plotted on the surface for adolescents born EPT, and adolescent born FT. Cooler blue colors indicate that a vertex is rarely a border of a network, where warmer red colors indicate a vertex is almost always a network boundary. **(b)** The mean times the vertices within a network (defined by the adolescent seven-network solution, x-axis) are a boundary across $k = 8$–25 networks (y-axis). Higher y-values indicate that a network is consistently subdivided across k. The darker bars correspond to the EPT group, and the lightly shaded bars correspond to the FT group. Error bars indicate standard error of the mean. $^{***}p < 0.001$.

for the EPT and FT groups. The dark red lines in the posterior cingulate cortex in both groups illustrate the qualitative finding above that a posterior cingulate network component emerges in the EPT group at higher k. The areas of blue in both groups across primary areas indicate that visual and sensorimotor clusters are particularly preserved across solutions. In both groups, the connectivity profiles of primary cortex are highly homogenous.

We then quantified how often a given network is subdivided in higher resolution solutions. Figure 4b displays the mean number of times a vertex is a boundary, averaging across all vertices belonging to each network identified in the optimal seven-network solution for a given group. Significant differences between groups were observed in the ventral attention [FT>EPT; two-sample t-test, $p = 1.17 \times 10^{-9}$, $t(5916) = -6.09$], somatomotor [FT>EPT; $p = 3.42 \times 10^{-9}$, $t(7103) = -5.92$], and default networks [EPT>FT; $p = 9.94 \times 10^{-20}$, $t(7562) = 9.36$]. These networks were the most different between groups in how frequently they were subdivided.

The ventral and default networks cover the frontoparietal cortex and are particularly interesting because EPT solutions were further subdivided within the default network (suggesting the EPT default network comprised more heterogeneous connectivity profiles) and FT is further subdivided for ventral (suggesting the FT ventral attention network comprised more heterogeneous connectivity profiles). In both groups (compared with all other networks), association networks (e.g., control and limbic networks) were further subdivided with higher k networks, that is, consisted of more heterogenous connectivity profiles in both EPT and FT.

Conversely, the somatomotor and visual networks (networks covering primary cortices) were subdivided the least, even with higher k. Note that because network labels are group-specific, the significant difference between groups for the somatomotor network (where the FT group had a

higher mean value) may be attributed to the insular component, which is included in the FT, but not the EPT, somatomotor network.

The main group differences in the seven-network solutions were in the insula and cingulate components. Do these differences persist across k? The insula and cingulate components were parts of larger (and different) networks in both groups, so to address the differences in these specific components for higher k, Figure 5 constrains the boundary analysis to anatomical regions of interest (ROIs) that cover these key areas. The regions were defined by the automated segmentation for the FreeSurfer5 template (Desikan et al., 2006). Note that unlike the above analysis, the search spaces (the nonblack regions in Fig. 5a) are the same across groups. First, we found that the insula was more parcellated in the FT solutions than in the EPT solutions [Fig. 5b; two-sample t-test-left: $p = 3.96 \times 10^{-4}$, $t(656) = 3.56$; right: $p = 0.0049$, $t(642) = 2.83$].

In other words, the connectivity profiles of the insular cortex were more homogeneous for the EPT adolescents than for FT adolescents *across* k, not just in the $k = 7$ solution. Second, none of the three anatomical regions selected to cover the PCC (bilateral posterior cingulate, precuneus, and isthmus cingulate) showed a significant difference between groups (Fig. 5b). In the FT seven-network solution, the connectivity profiles of these vertices were so similar to each other that they formed their own network (the FT proto-limbic network). In contrast, for the EPT seven-network solution, the connectivity of these vertices was not distinct enough compared with other areas of the cortex, and the posterior cingulate cortex was subsumed by the default mode network (resulting in a between-group difference).

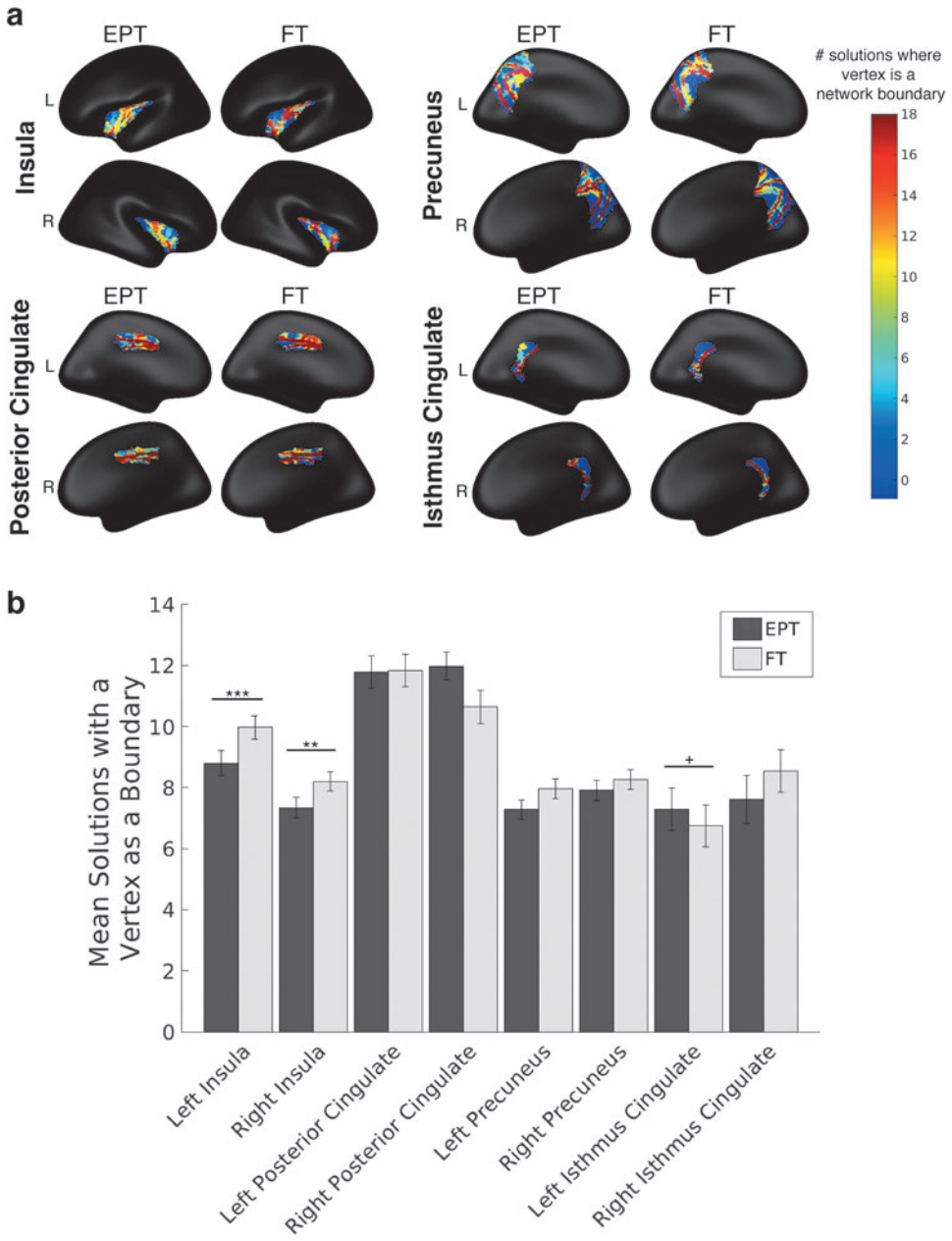

FIG. 5. Differences in subdivisions in anatomical ROIs. **(a)** Surface plots showing Figure 4a within anatomical ROIs identified as having key group differences in the optimal seven-network solution. The same color scale is used for all regions and black indicates vertices not within the ROI. **(b)** Bar plot of the mean times a vertex within the ROI is a network boundary. Darker bars denote the EPT group, lighter bars denote the FT group, and the error bars show the standard error of the mean. $^{+}p < 0.1$, $^{**}p < 0.01$, and $^{***}p < 0.001$. ROI, region of interest.

However, when we looked at $k > 7$ networks, there is no longer a group difference—this result supports what we saw qualitatively in Supplementary Figure S1 where an analogous posterior cingulate network component emerges with higher k in the EPT group. This suggests that the insula component is consistently different from the FT group, regardless of the k selected, and is perhaps a more meaningful and robust difference in functional organization between groups.

Comparison with adult organization

We separately compared the $k = 7$-network solution for the EPT and FT adolescent groups with the seven-network solution reported from a large sample of adult resting-state data (Yeo et al., 2011). Figure 6a displays the adult seven-network solution and the adolescent seven-network solutions, recolored based on pairing the adolescent networks with the adult networks without replacement. Averaging across networks, we found that the EPT and FT groups had similar overlap to adults with Dice coefficients of 0.6985 for EPT and 0.7004 for FT. However, Figure 6b reveals some interesting group differences that emerge when the overlap is broken up by network. In both groups, the visual network was the most similar to the adult solution.

The key difference between the two groups was in the limbic network (named from the Yeo et al, 2011 atlas) in which the preterm solution had significantly more overlap to the adult solution [$t(47.80) = -61.22$, $p = 4.55 \times 10^{-47}$]. This suggests that the limbic network in EPT adolescents is more adultlike than in FT adolescents.

Because of the prevalence of individual differences in resting-state networks, we also compared individualized solutions within each group with the adult networks. Representative individual solutions are shown in Figure 7a. Figure 7b compares the distribution of each adult network's overlap with individual adolescent solutions, broken up by group. As expected, the overlap between a subject's limbic network and the adult limbic network yielded the largest difference between groups [EPT mean: 0.18, FT mean: 0.07; $t(21.02) = 3.91$, $p = 8 \times 10^{-4}$]. There was a trend toward a difference in the overlap to the somatomotor network [EPT mean: 0.55, FT mean: 0.64; $t(35.95) = -1.93$, $p = 0.06$], but the group differences in overlap for all other networks were not significant (all $p > 0.3$).

Predicting cognition from limbic network maturity

Finally, we conducted an exploratory analysis to test whether an individual's similarity to adult networks corresponds to performance on the NIH Toolbox Cognition Battery. The composite score for cognition was significantly different between groups [FT group mean = 109.46, EPT group mean = 84.86, $t(45.91) = 5.57$, $p = 1.28 \times 10^{-6}$; Fig. 8a]. This relationship is expected, based on the extensive research showing deficits in cognitive performance throughout the life span attributed to preterm birth. However, how does maturity of functional networks relate to these behavioral differences?

To answer this question, we tested if overlap to the adult limbic network is predictive of cognition. We chose to focus on the limbic network, as it consistently yielded the largest differences between the FT and EPT groups. A model with main effects of group and individual limbic network overlap with adults can predict the overall age-corrected cognition [$p = 5.395 \times 10^{-5}$, $F(3,38) = 10.01$], explaining 39.7% of the variance (adjusted $R^2 = 0.3972$, multiple $R^2 = 0.4413$). The estimates for all predictors are summarized in Table 2. Figure 8b shows the marginal effects of the group and limbic overlap interaction. The FT group has a higher slope, where increases in limbic overlap are associated with higher overall cognition, whereas increases in limbic overlap are associated with lower overall cognition in

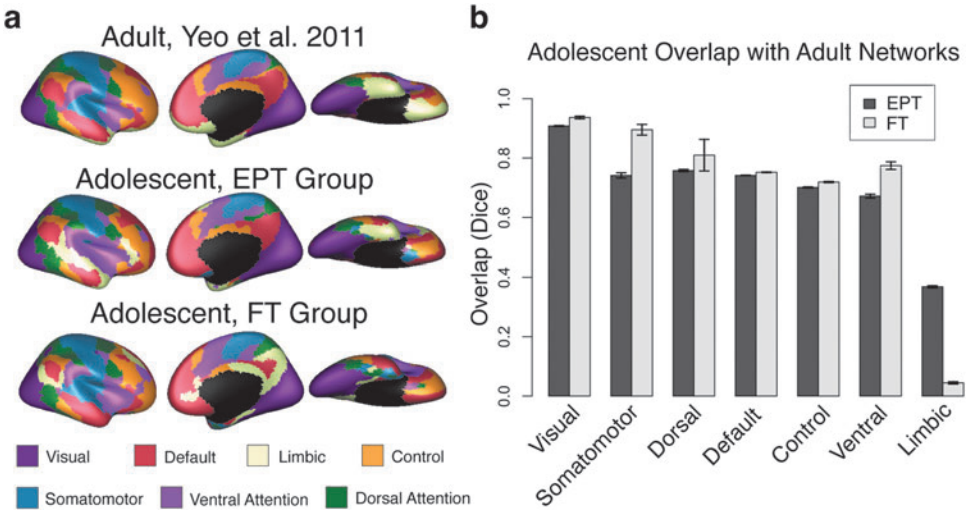

FIG. 6. Comparison with adult networks. **(a)** The seven-network solutions for adults (from Yeo et al., 2011), adolescents born EPT, and adolescents born FT are plotted on the surface. The color scheme is adopted from Yeo et al. (2011). Adolescent networks are matched to an adult network based on overlap (without replacement). **(b)** Comparison of adolescent networks with adult networks (plotted on x-axis) quantified by Dice index of overlap (y-axis). Higher Dice indicates higher overlap. The darker bars correspond to the EPT group, and the lightly shaded bars correspond to the FT group. Error bars indicate standard error of the mean, from the Dice of the $N - 1$ solutions.

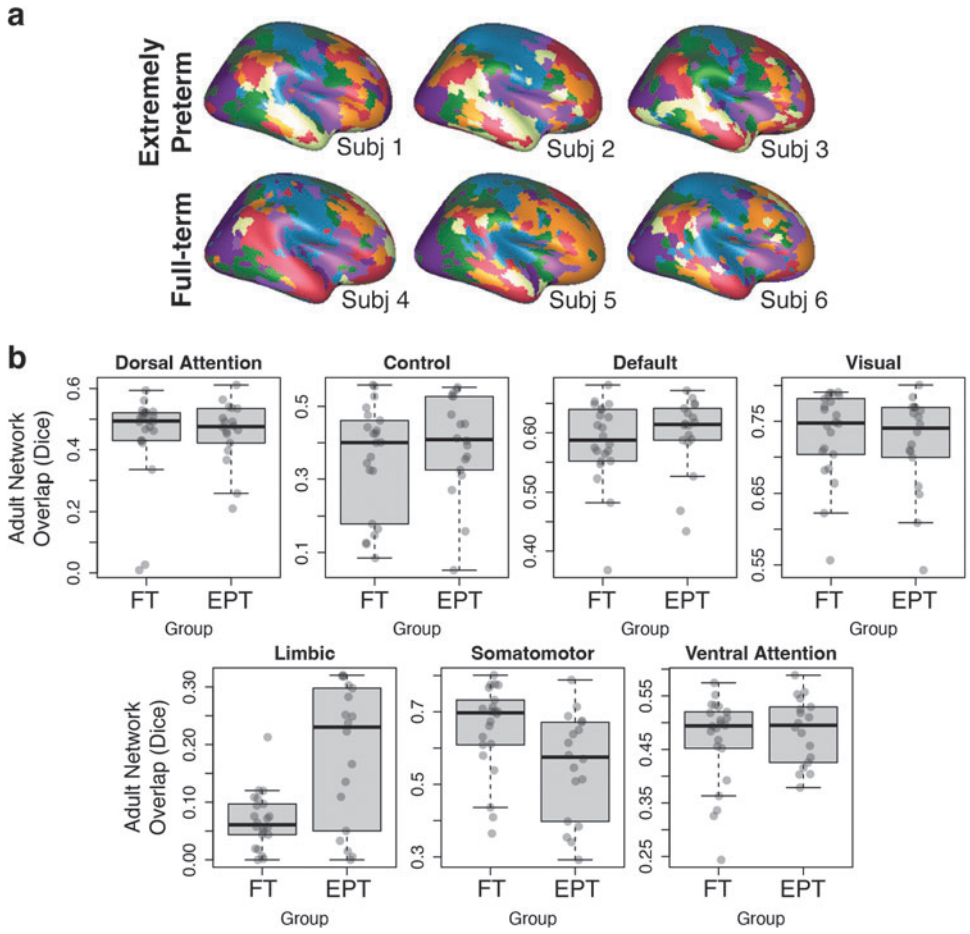

FIG. 7. Individual overlap with adult networks. **(a)** Examples of subject-level parcellations calculated using k-NN assignment to group centroids. **(b)** Boxplots of individual solution overlap (quantified using Dice) with each adult network broken up by group (FT, EPT). Overlaid points indicate single subjects.

the preterm group (interaction effect of limbic overlap and preterm birth: $p = 0.058$).

These results are replicated when including the full group (without removing the eight noisier individual solutions; Supplementary Table S3 and Supplementary Fig. S6). Because there was a significant difference in socioeconomic status (SES) between groups, we explored adding a main effect of SES to the model, but found that the reduced model (i.e., no term for SES) was preferred ($BIC_{full} = 364.78 > BIC_{reduced} = 364.61$). While a larger sample size may better

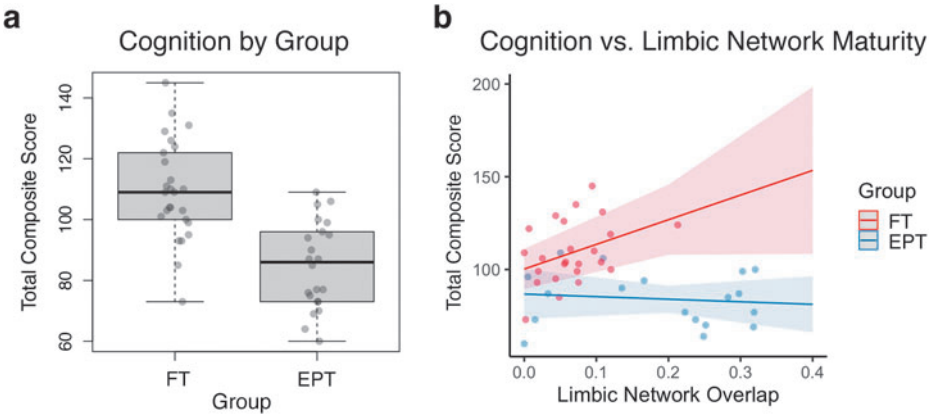

FIG. 8. Predicting cognition. **(a)** Boxplots of the cognition total composite score broken up by group (FT, EPT). The overlaid points indicate individual subjects. **(b)** Scatterplot of the cognition total composite score versus limbic network overlap (Dice index). Higher Dice indicates higher overlap with the adult limbic network. Each point indicates an individual subject, where red points are FT subjects and blue points are EPT subjects. The lines correspond to the regression model's predicted values of total cognition scores from limbic network overlap within each group, with 95% confidence regions.

Table 2. Predicting Total Cognition from Group and Limbic Overlap

Coefficients	*Estimate*	*Standard error*	*t*	*p*
Limbic overlap	132.848	68.129	1.950	0.0586
EPT group	−13.486	8.812	−1.530	0.1342
Limbic × preterm interaction	−146.690	75.009	−1.956	0.0579

Overall model fit: $F(3,38) = 10.01$, adjusted $R^2 = 0.3972$, $p = 5.395 \times 10^{-5}$.

elucidate this brain–behavior relationship, these results provide evidence that brain maturity (as measured by an adolescent's proto-limbic network) can explain individual differences in cognition beyond using only GA at birth.

Discussion

In this study, we parcellated resting-state connectomes for adolescents born EPT and a comparison group of adolescents born FT to measure broadscale functional organization. We used an unsupervised learning technique to parcellate vertices into networks based on the similarities of their whole-brain connectivity profiles. A seven-network parcellation was found to be optimal for both groups of adolescents based on fit to left-out individuals and stability of solutions. Using these optimal parcellations, we identified group-level differences, computed group-informed subject-level parcellations, compared adolescent parcellations with adult parcellations, and explored how maturity of resting-state networks corresponded to behavior.

First, while most networks were highly similar for the EPT and FT groups (also reflected in the overall Dice overlap between groups), the EPT parcellation included an insular component, whereas the FT parcellation included a PCC component that was differentiated from other networks. Previous work in adolescents born preterm identified reduced gray matter volume in the insula (Karolis et al., 2017; Nosarti et al., 2008) and disruptions in functional connectivity of the salience (or ventral attention) network, including the insula (Degnan et al., 2015; Wehrle et al., 2018). The structural contributions of the PCC in adolescents born preterm are less clear.

In adolescents born VPT, Karolis et al. (2017) found a significant reduction in gray matter volume (compared with FT adolescents) for the anterior cingulate cortex (ACC), but not the PCC, whereas Nosarti et al. (2008) found a significant *increase* in GM for the ACC and PCC. In addition, seed-based functional connectivity analyses have found hyperconnectivity in adolescents born late preterm (Degnan et al., 2015), but no group differences in networks seeding PCC were found in adolescents born VPT (Wehrle et al., 2018). One advantage of our vertex-based approach of whole-brain connectivity is that it can distinguish differences in both short- and long-range connections that may not be discernible using previous, for example, independent component analysis-based or ROI-based, network-level analyses.

However, while we see major differences in the insula, we still observed other differences in network assignment across the cortex, which is in line with previous work showing global differences in functional connectivity in adolescents born preterm (Degnan et al., 2015; Wehrle et al., 2018). Exploring the boundaries across all k allows further insight into differences in functional organization. In both groups, the primary cortex was often undivided across k, suggesting more homogenous connectivity profiles, whereas the association networks were further subdivided in higher k solutions. Critically, when focusing on specific anatomical regions, only the insula remained a consistent group difference across k, suggesting it is a more robust difference than the PCC.

Our comparisons with adult networks revealed that while the EPT group showed some overlap with the adult limbic network particularly in the inferior temporal lobe, the FT group's networks had very little overlap with the adult limbic network. To our knowledge, networks for adolescents born EPT or FT have not been compared with the adult (Yeo et al., 2011) networks, but the immaturity of the limbic network has been previously reported in adolescents (Dong et al., 2021; Váša et al., 2020). Dong et al. (2021) and Vasa et al. (2020) use different methods and are not parcellation approaches, but overall, they find a similar pattern: faster maturity in the primary areas and later maturity of association areas. Also, work in FT neonates has shown lack of a differentiated limbic network (Molloy and Saygin, 2022).

The current finding is thus consistent with previous literature in suggesting that prolonged maturity of the limbic network may be an important aspect of typical development. Despite well-documented brain-wide disruptions, the EPT parcellation yielded a more adultlike limbic network, suggesting accelerated development of the limbic network.

Evidence for accelerated development was also observed in the brain-wide confidence, where the precuneus and temporal parietal junction confidences were more adultlike (Yeo et al., 2011) in EPT adolescents and more childlike (Tooley et al., 2022) in FT adolescents. In other studies, this accelerated development has been reported in the structure of adolescents born EPT, who have higher maturational indices in gray matter volume (Karolis et al., 2017). This may also indicate that some critical aspects of limbic integration with other networks in FT adolescents are absent in EPT born youth (Blakemore and Mills, 2014; Casey, 2015; Crone and Dahl, 2012).

A study of the mentalizing network in the present sample of adolescents found that the largest differences between EPT and FT adolescents were in gray matter volume and surface area in the temporal lobe (Fu et al., 2022). Findings from these two studies suggest that the temporal lobe is a key component of group differences in terms of both structure and function.

Interestingly, we found a relationship between network maturity and cognition, where more precocious, or adultlike, development of the limbic network was associated with higher cognitive scores in the FT group. For the adolescents born EPT, the relationship between limbic overlap and cognitive scores was weaker, but importantly, limbic overlap

was much lower for the FT group, with only the EPT group showing Dice overlap >0.2 with the adult limbic network (i.e., greater similarity to adults). Thus, accelerated limbic development in EPT is not associated with more advanced cognitive development. It is possible that EPT and FT adolescents show different susceptibility for experiential inputs, or perhaps they are in a different stage of development. For example, there may be a plateau in cortical development where accelerated brain development is no longer advantageous for cognition (as we observed for EPT).

Subcortical development may also provide additional information for assessing the relationship between network maturity and cognition. Indeed, an important limitation of the Yeo seven-network approach (and our comparison to it) is that subcortical structures such as the amygdala, hippocampus, and striatum, which are strongly interconnected with regions of the temporal lobe and orbitofrontal cortex that comprise the Yeo limbic network, are not included in the parcellation.

While the present study uses resting-state fMRI, previous task-based fMRI studies on the insula, PCC, and limbic network may give us insight into the nature of the group differences we observe. The insula is involved in social processing as well as high-level attention (Uddin et al., 2017), as is the PCC (especially as part of the default mode network) (Leech and Sharp, 2014), and the differences we observe here may underlie some of the behavioral differences observed between groups in these domains (Taylor, 2020).

The limbic network in adults is involved in emotion, reward, and associative learning (Rolls, 2019; Yeo et al., 2015). The broad functional scope of the limbic network may explain the diverse group differences in behavior and cognition observed in children and adults born EPT. While the subcortical regions were not included in this analysis, the relationship between this network and subcortical regions may suggest a potential mechanism for limbic network development. In typically developing children, fMRI studies have demonstrated that subcortical structures of the limbic networks play a role in guiding cognition, decision-making, and behavior in adolescence, and potentially also impact maturation and function of *cortical* brain circuits in adulthood (Casey, 2015; Crone and Dahl, 2012; Davidow et al., 2018; Nelson et al., 2014).

The absence of prolonged development of the cortical limbic network and other neural signatures we observe in adolescents born FT suggest that perhaps motivational and value-based inputs of subcortical areas guide behavior and ultimately shape the maturation of cortical limbic circuitry in typical development, and that this may be an important missing element of EPT neurobehavioral development (Fareri et al., 2015; Gabard-Durnam et al., 2014; Johns et al., 2019). When viewed in the context of these previous models, our data suggest that cortical limbic network development may not undergo the same process in EPT adolescents. This interpretation echoes previous findings in adolescents showing a relationship between brain structure and IQ (Cheong et al., 2013; Karolis et al., 2017).

Future work is needed to replicate the relationship between limbic maturity and cognitive ability in a larger sample of adolescents. Also, we used the overlap of the entire limbic network, to reduce the number of regressors and avoid overfitting the model, but this summary statistic does not tell us which connections within that network are most predictive of higher cognitive ability, or if connections outside of the limbic network may be more predictive. Previous research showed limited evidence of any relationship of specific between-network structural or functional connectivity and behavior (Degnan et al., 2015; Wehrle et al., 2018), and so, this overlap measure computed from the entire connectome may in fact be more informative than between-network connections.

However, there is also evidence that cognition is best predicted by thalamocortical connections (Ball et al., 2015), or frontal connections (Girault et al., 2019), and so, the use of specific connections versus overall broadscale organization to predict cognition remains an open question warranting future investigation.

There are many unanswered questions about the emergence of these network-level differences and their relationship to the broad behavioral and cognitive outcomes associated with preterm birth. Longitudinal characterization of an individual's functional organization may identify if there was a point where these differences become negligible. In addition, exploring specific behavioral measures instead of overall cognition could identify which domains (e.g., executive function, working memory) are most closely related to these markers of brain organization. A larger sample size would likely improve the accuracy and generalizability of the linear model, allowing for more robust predictions of behavior.

Another limitation is the relationship between socioeconomic status and preterm birth, which remains a confound in this study and studies of preterm birth in general. Our analysis indicated that including SES into the predictive model did not improve the fit enough to counteract the added complexity, but previous work has demonstrated an additive effect of preterm birth and SES on predicting cognitive development (Beauregard et al., 2018). Larger sample sizes spanning a larger distribution of SES will better address the effects of SES and preterm birth on development. Finally, we only explored cortical parcellations, which is in line with the numerous adult parcellation approaches, and best matches our comparison with the Yeo et al. (2011) network parcellation.

Future work can explore subcortical connectivity as well, which would also be informative for delving deeper into the limbic network differences we find here, given that a large portion of the limbic network is actually subcortical.

Conclusion

Broadscale differences in functional organization revealed by resting-state fMRI are present in adolescents born EPT compared with adolescents born FT. These differences are brain wide, with the largest differences in insular and limbic networks. Adolescents born EPT show a more adultlike limbic network, and an individual's overlap with the adult limbic network may be a predictor of their overall cognitive ability.

Data Availability Statement

The authors will work to make fully deidentified data available to investigators if legal requirements can be met.

Acknowledgment

Analyses were completed using the Ohio Supercomputer.

Authors' Contributions

M.F.M.: Writing—original draft (lead), conceptualization (equal), visualization (lead), formal analysis (lead), methodology (lead), and software (lead). E.J.Y.: Formal analysis (support), software (support), and writing—review and editing (equal). W.I.M.: Investigation (equal) and writing—review and editing (equal). K.R.H.: Investigation (equal) and writing—review and editing (equal). H.G.T.: Investigation (equal), funding acquisition (equal), and writing—review and editing (equal). D.E.O.: Formal analysis (support), software (support), and writing—review and editing (equal). E.E.N.: Investigation (equal), supervision (support), writing—review and editing (equal), and funding acquisition (equal). Z.M.S.: Conceptualization (equal), writing—original draft (support), methodology (support), supervision (lead), and funding acquisition (equal).

Author Disclosure Statement

No competing financial interests exist.

Funding Information

This research was partly funded by the Alfred P. Sloan Foundation (to Zeynep M. Saygin), Ohio State's Chronic Brain Injury Program (to Zeynep M. Saygin), Ohio State University's College of Arts and Sciences (to Zeynep M. Saygin and M. Fiona Molloy) and College of Engineering (to Emily J. Yu), and the Abigail Wexner Research Institute of Nationwide Children's Hospital to H. Gerry Taylor and Eric E. Nelson.

Supplementary Material

Supplementary Figure S1
Supplementary Figure S2
Supplementary Figure S3
Supplementary Figure S4
Supplementary Figure S5
Supplementary Figure S6
Supplementary Table S1
Supplementary Table S2
Supplementary Table S3

References

Aarnoudse-Moens CSH, Weisglas-Kuperus N, van Goudoever JB, et al. Meta-analysis of neurobehavioral outcomes in very preterm and/or very low birth weight children. Pediatrics 2009;124(2):717–728; doi: 10.1542/peds.2008-2816

Anderson PJ, Cheong JLY, Thompson DK. The predictive validity of neonatal MRI for neurodevelopmental outcome in very preterm children. Semin Perinatol 2015;39(2):147–158; doi: 10.1053/j.semperi.2015.01.008

Anderson PJ, de Miranda DM, Albuquerque MR, et al. Psychiatric disorders in individuals born very preterm/very low-birth weight: An individual participant data (IPD) meta-analysis. EClinicalMedicine 2021;42:101216; doi: 10.1016/j.eclinm.2021.101216

Anjari M, Srinivasan L, Allsop JM, et al. Diffusion tensor imaging with tract-based spatial statistics reveals local white matter abnormalities in preterm infants. Neuroimage 2007;35(3):1021–1027; doi: 10.1016/j.neuroimage.2007.01.035

Arslan S, Ktena SI, Makropoulos A, et al. Human brain mapping: A systematic comparison of parcellation methods for the human cerebral cortex. Neuroimage 2018;170:5–30; doi: 10.1016/j.neuroimage.2017.04.014

Ball G, Aljabar P, Zebari S, et al. Rich-club organization of the newborn human brain. Proc Natl Acad Sci U S A 2014;111(20):7456–7461; doi: 10.1073/pnas.1324118111

Ball G, Boardman JP, Aljabar P, et al. The influence of preterm birth on the developing thalamocortical connectome. Cortex 2013;49(6):1711–1721; doi: 10.1016/j.cortex.2012.07.006

Ball G, Pazderova L, Chew A, et al. Thalamocortical connectivity predicts cognition in children born preterm. Cereb Cortex 2015;25(11):4310–4318; doi: 10.1093/cercor/bhu331

Batalle D, Hughes EJ, Zhang H, et al. Early development of structural networks and the impact of prematurity on brain connectivity. Neuroimage 2017;149:379–392; doi: 10.1016/j.neuroimage.2017.01.065

Beauregard JL, Drews-Botsch C, Sales JM, et al. Preterm birth, poverty, and cognitive development. Pediatrics 2018;141(1):e20170509; doi: 10.1542/peds.2017-0509

Blakemore S-J, Mills KL. Is adolescence a sensitive period for sociocultural processing? Annu Rev Psychol 2014;65:187–207; doi: 10.1146/annurev-psych-010213-115202

Buckholtz JW and Meyer-Lindenberg A. psychopathology and the human connectome: Toward a transdiagnostic model of risk for mental illness. Neuron 2012;74(6):990–1004; doi: 10.1016/j.neuron.2012.06.002

Casaletto KB, Umlauf A, Beaumont J, et al. Demographically corrected normative standards for the english version of the NIH toolbox cognition battery. J Int Neuropsychol Soc 2015;21(5):378–391; doi: 10.1017/S1355617715000351

Casey BJ. Beyond simple models of self-control to circuit-based accounts of adolescent behavior. Annu Rev Psychol 2015;66(1):295–319; doi: 10.1146/annurev-psych-010814-015156

Cheong JLY, Anderson PJ, Roberts G, et al. Contribution of brain size to IQ and educational underperformance in extremely preterm adolescents. PLoS One 2013;8(10):e77475; doi: 10.1371/journal.pone.0077475

Collins SE, Thompson DK, Kelly CE, et al. Development of regional brain gray matter volume across the first 13 years of life is associated with childhood math computation ability for children born very preterm and full term. Brain Cogn 2022;160:105875; doi: 10.1016/j.bandc.2022.105875

Crone EA, Dahl RE. Understanding adolescence as a period of social–affective engagement and goal flexibility. Nat Rev Neurosci 2012;13(9):636–650; doi: 10.1038/nrn3313

Damaraju E, Phillips J, Lowe JR, et al. Resting-state functional connectivity differences in premature children. Front Syst Neurosci 2010;4:23; doi: 10.3389/fnsys.2010.00023

Davidow JY, Insel C, Somerville LH. Adolescent development of value-guided goal pursuit. Trends Cogn Sci 2018;22(8):725–736; doi: 10.1016/j.tics.2018.05.003

de Almeida JS, Meskaldji DE, Loukas S, et al. Preterm birth leads to impaired rich-club organization and fronto-paralimbic/limbic structural connectivity in newborns. Neuroimage 2020;225:117440–117440; doi: 10.1016/j.neuroimage.2020.117440

Degnan AJ, Wisnowski JL, Choi S, et al. Altered structural and functional connectivity in late preterm preadolescence: An anatomic seed-based study of resting state networks related to the posteromedial and lateral parietal cortex. PLoS One 2015;10(6):e0130686; doi: 10.1371/journal.pone.0130686

Desikan RS, Ségonne F, Fischl B, et al. An automated labeling system for subdividing the human cerebral cortex on MRI

scans into gyral based regions of interest. Neuroimage 2006; 31(3):968–980; doi: 10.1016/j.neuroimage.2006.01.021

Dice LR. Measures of the amount of ecologic association between species. Ecology 1945;26(3):297–302; doi: 10.2307/1932409

Dimitrova R, Arulkumaran S, Carney O, et al. Phenotyping the preterm brain: Characterizing individual deviations from normative volumetric development in two large infant cohorts. Cereb Cortex 2021;31(8):3665–3677; doi: 10.1101/2020.08.05.228700

Dong H-M, Margulies DS, Zuo X-N, et al. Shifting gradients of macroscale cortical organization mark the transition from childhood to adolescence. Proc Natl Acad Sci U S A 2021; 118(28):e2024448118; doi: 10.1073/pnas.2024448118

Doria V, Beckmann CF, Arichi T, et al. Emergence of resting state networks in the preterm human brain. Proc Natl Acad Sci U S A 2010;107(46):20015–20020; doi: 10.1073/pnas.1007921107

Eickhoff SB, Yeo BTT, Genon S. Imaging-based parcellations of the human brain. Nat Rev Neurosci 2018;19(11):672–686; doi: 10.1038/s41583-018-0071-7

Eyre M, Fitzgibbon SP, Ciarrusta J, et al. The developing human connectome project: Typical and disrupted perinatal functional connectivity. Brain 2021;144(7):2199–2213; doi: 10.1093/brain/awab118

Fareri DS, Gabard-Durnam L, Goff B, et al. Normative development of ventral striatal resting state connectivity in humans. Neuroimage 2015;118:422–437; doi: 10.1016/j.neuroimage.2015.06.022

Fränti P, Sieranoja S. How much can k-means be improved by using better initialization and repeats? Pattern Recognit 2019;93:95–112; doi: 10.1016/j.patcog.2019.04.014

Fu X, Hung A, de Silva AD, et al. Development of the mentalizing network structures and theory of mind in extremely preterm youth. Soc Cogn Affect Neurosci 2022;17(11):977–985; doi: 10.1093/scan/nsac027

Gabard-Durnam LJ, Flannery J, Goff B, et al. The development of human amygdala functional connectivity at rest from 4 to 23 years: A cross-sectional study. Neuroimage 2014;95:193–207; doi: 10.1016/j.neuroimage.2014.03.038

Girault JB, Munsell BC, Puechmaille D, et al. White matter connectomes at birth accurately predict cognitive abilities at age 2. Neuroimage 2019;192:145–155; doi: 10.1016/j.neuroimage.2019.02.060

Heinonen K, Eriksson JG, Lahti J, et al. Late preterm birth and neurocognitive performance in late adulthood: A birth cohort study. Pediatrics 2015;135(4):e818–e825; doi: 10.1542/peds.2014-3556

Inder TE, Warfield SK, Wang H, et al. Abnormal cerebral structure is present at term in premature infants. Pediatrics 2005; 115(2):286–294; doi: 10.1542/peds.2004-0326

Johns CB, Lacadie C, Vohr B, et al. Amygdala functional connectivity is associated with social impairments in preterm born young adults. Neuroimage Clin 2019;21:101626; doi: 10.1016/j.nicl.2018.101626

Johnson S, Marlow N. Early and long-term outcome of infants born extremely preterm. Arch Dis Child 2017;102(1):97–102; doi: 10.1136/archdischild-2015-309581

Karolis VR, Froudist-Walsh S, Kroll J, et al. Volumetric grey matter alterations in adolescents and adults born very preterm suggest accelerated brain maturation. Neuroimage 2017;163: 379–389; doi: 10.1016/j.neuroimage.2017.09.039

Kerr-Wilson CO, Mackay DF, Smith GCS, et al. Meta-analysis of the association between preterm delivery and intelligence. J Public Health 2012;34(2):209–216; doi: 10.1093/pubmed/fdr024

Kong R, Li J, Orban C, et al. Spatial topography of individual-specific cortical networks predicts human cognition, personality, and emotion. Cereb Cortex 2019;29(6):2533–2551; doi: 10.1093/cercor/bhy123

Leech R, Sharp DJ. The role of the posterior cingulate cortex in cognition and disease. Brain 2014;137(1):12–32; doi: 10.1093/brain/awt162

Molloy MF, Saygin ZM. Individual variability in functional organization of the neonatal brain. Neuroimage 2022;253: 119101; doi: 10.1016/j.neuroimage.2022.119101

Moster D, Lie RT, Markestad T. Long-term medical and social consequences of preterm birth. N Engl J Med 2008;359(3): 262–273; doi: 10.1056/NEJMoa0706475

Nelson EE, Lau JYF, Jarcho JM. Growing pains and pleasures: How emotional learning guides development. Trends Cogn Sci 2014;18(2):99–108; doi: 10.1016/j.tics.2013.11.003

Nosarti C, Giouroukou E, Healy E, et al. Grey and white matter distribution in very preterm adolescents mediates neurodevelopmental outcome. Brain 2008;131(Pt 1):205–217; doi: 10.1093/brain/awm282

Nosarti C, Nam KW, Walshe M, et al. Preterm birth and structural brain alterations in early adulthood. Neuroimage Clin 2014;6:180–191; doi: 10.1016/j.nicl.2014.08.005

Orchinik LJ, Taylor HG, Espy KA, et al. Cognitive outcomes for extremely preterm/extremely low birth weight children in kindergarten. J Int Neuropsychol Soc 2011;17(6):1067–1079; doi: 10.1017/S135561771100107X

Pascoe L, Burnett AC, Anderson PJ. Cognitive and academic outcomes of children born extremely preterm. Semin Perinatol 2021;45(8):151480; doi: 10.1016/j.semperi.2021.151480

Pesonen A-K, Räikkönen K, Heinonen K, et al. Personality of young adults born prematurely: The Helsinki study of very low birth weight adults. J Child Psychol Psychiatry 2008; 49(6):609–617; doi: 10.1111/j.1469-7610.2007.01874.x

Pineda R, Liszka L, Tran P, et al. Neurobehavior in very preterm infants with low medical risk and full-term infants. J Perinatol 2022;42(10):1400–1408; doi: 10.1038/s41372-022-01432-3

Rolls ET. The cingulate cortex and limbic systems for emotion, action, and memory. Brain Struct Funct 2019;224(9):3001–3018; doi: 10.1007/s00429-019-01945-2

Rosenberg MD, Finn ES, Scheinost D, et al. A neuromarker of sustained attention from whole-brain functional connectivity. Nat Neurosci 2016;19(1):165–171; doi: 10.1038/nn.4179

Scheinost D, Kwon SH, Shen X, et al. Preterm birth alters neonatal, functional rich club organization. Brain Struct Funct 2016;221(6):3211–3222; doi: 10.1007/s00429-015-1096-6

Schnider B, O'Gorman RL, Tuura RO, et al. Altered brain metabolism contributes to executive function deficits in school-aged children born very preterm. Pediatr Res 2020;88(5): 739–748; doi: 10.1038/s41390-020-1024-1

Schwarz G. Estimating the dimension of a model. Ann Statist 1978;6(2):461–464; doi: 10.1214/aos/1176344136

Taylor HG. Neurodevelopmental origins of social competence in very preterm children. Semin Fetal Neonatal Med 2020; 25(3):101108; doi: 10.1016/j.siny.2020.101108

Tooley UA, Bassett DS, Mackey AP. Functional brain network community structure in childhood: Unfinished territories and fuzzy boundaries. Neuroimage 2022;247:118843; doi: 10.1016/j.neuroimage.2021.118843

Uddin LQ, Nomi JS, Hebert-Seropian B, et al. Structure and function of the human insula. J Clin Neurophysiol 2017; 34(4):300–306; doi: 10.1097/WNP.0000000000000377

van den Heuvel MP and Sporns O. A cross-disorder connectome landscape of brain dysconnectivity. Nature Reviews Neuroscience 2019;20(7):435–446; doi: 10.1038/s41583-019-0177-6

Váša F, Romero-Garcia R, Kitzbichler MG, et al. Conservative and disruptive modes of adolescent change in human brain functional connectivity. Proc Natl Acad Sci U S A 2020; 117(6):3248–3253; doi: 10.1073/pnas.1906144117

Wehrle FM, Michels L, Guggenberger R, et al. Altered resting-state functional connectivity in children and adolescents born very preterm. Neuroimage Clin 2018;20:1148–1156; doi: 10.1016/j.nicl.2018.10.002

Yeo BT, Krienen FM, Sepulcre J, et al. The organization of the human cerebral cortex estimated by intrinsic functional connectivity. J Neurophysiol 2011;106(3):1125–1165; doi: 10.1152/jn.00338.2011

Yeo BTT, Krienen FM, Eickhoff SB, et al. Functional specialization and flexibility in human association cortex. Cereb Cortex 2015;25(10):3654–3672; doi: 10.1093/cercor/bhu217

Address correspondence to:
Zeynep M. Saygin
Department of Psychology
The Ohio State University
1835 Neil Avenue
Columbus, OH 43210
USA

E-mail: saygin.3@osu.edu